# Supplementary Material for "A model-based analysis of metal fate in the Thames Estuary"

**Valentina Premier · Anderson Abel de Souza Machado · Steve Mitchell · Christiane Zarfl · Kate Spencer · Marco Toffolon**

## 1 Discretization of the Thames Estuary

### 1.1 Computational domain

The grid was composed of 913×57 horizontal cells with 6852 active grid elements per layer, and 15 vertical layers. The cell area varies upstream to downstream from 300 to 170,000 $m^2$. The computational grid is shown in Figure 1. Figure 2 shows a detail of the bathymetry in the outer part of the Thames estuary.

Valentina Premier
Department of Civil, Environmental and Mechanical Engineering, University of Trento, Trento, Italy
Leibniz-Institute of Freshwater Ecology and Inland Fisheries, Berlin, Germany
Tel.: +39-0461-282480
Fax: +39-0461-282672
E-mail: valentina.premier@unitn.it

Anderson Abel de Souza Machado
Leibniz-Institute of Freshwater Ecology and Inland Fisheries, Berlin, Germany
Department of Biology, Chemistry, and Pharmacy, Freie Universität Berlin, Berlin, Germany
School of Geography, Queen Mary University of London, London, UK
E-mail: machado@igb-berlin.de

Steve Mitchell
School of Civil Engineering and Surveying, University of Portsmouth, Portsmouth, UK
E-mail: steve.mitchell@port.ac.uk

Christiane Zarfl
Center for Applied Geosciences, Eberhard Karls Universität Tübingen, Tübingen, Germany
E-mail: christiane.zarfl@uni-tuebingen.de

Kate Spencer
School of Geography, Queen Mary University of London, London, UK
E-mail: k.spencer@qmul.ac.uk

Marco Toffolon
Department of Civil, Environmental and Mechanical Engineering, University of Trento, Trento, Italy
E-mail: marco.toffolon@unitn.it

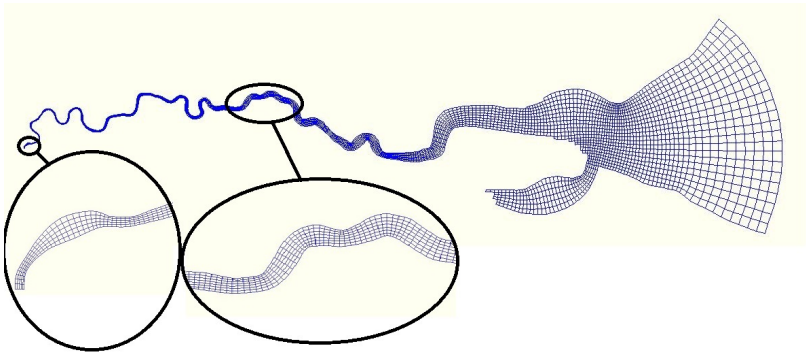

**Fig. 1** Details of the computational grid.

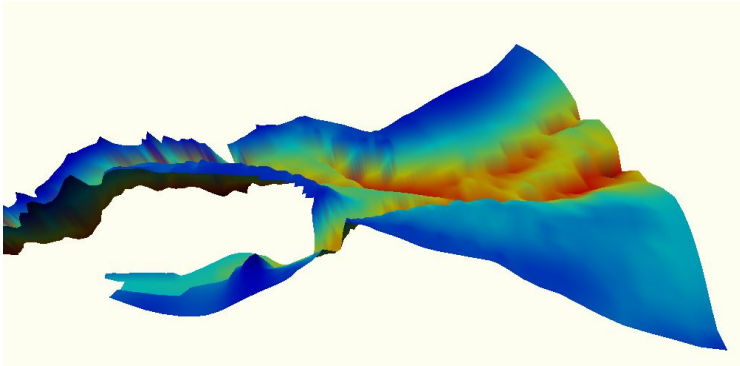

**Fig. 2** Details of the bathymetry in the outer part of the Thames estuary.

In order to compare the model results with the available measurements, observation points were created in the model where tidal gauges or water quality points were present throughout the estuary (Figure 1 in the main text).

## 1.2 Initial and boundary conditions

The seaward boundary condition was set up using the water level time series derived by the International Hydrographic Organization (IHO) using astronomical tidal constituents in Shivering Sands. Figure 3 shows the correlation with the water levels measured in Sheerness, highlighting the effect of storm surges. The discharges and the water level used as boundary conditions for the numerical model are shown in Figure 4, and the main statistics are reported in the main text (Table 1).

The weirs within the estuary were not simulated, but the absence of significant effects was tested running a simulation with a barrier, which is represented in the model by setting horizontal velocities at the position of the gate equal to zero. First, half a month was run without the gate, then the gate was inserted for 5 hours during a period of high water, according to an operational closure controlled by the Environmental Agency. After 5 hours, the rest of the month was run without the barrier. No differences were observed in salinity, water level and velocity envelopes.

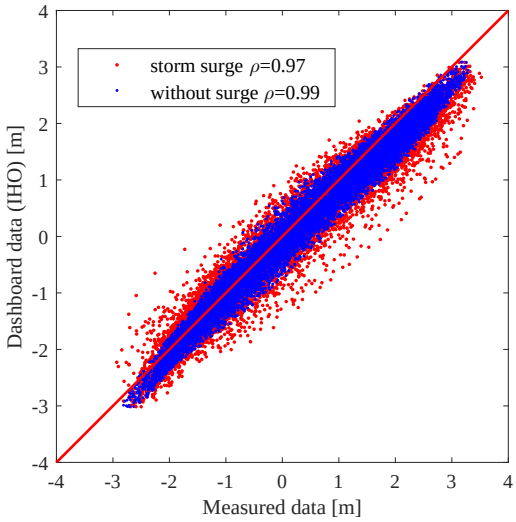


**Fig. 3** Scatter plot between astronomic water level prediction (IHO) and measured water levels in Sheerness. Red dots represent measurements characterized by storm surges.

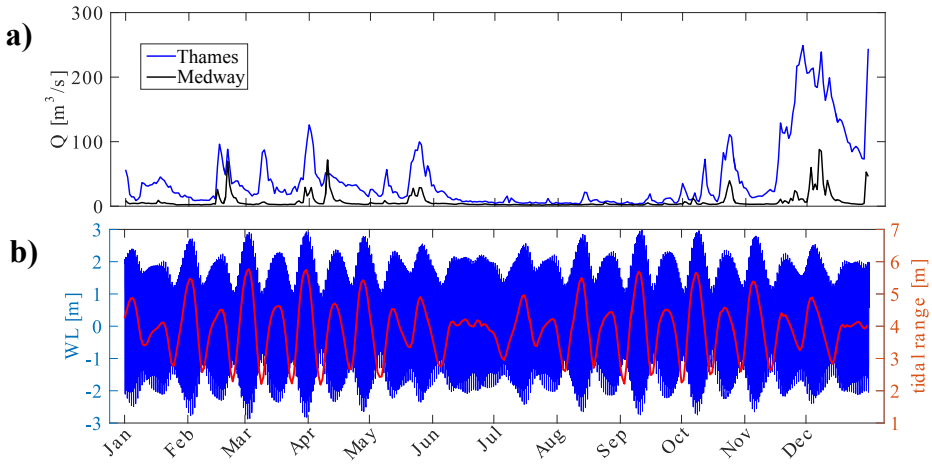


**Fig. 4** Boundary conditions used in the model for the year 2006: (a) discharges of the Thames and Medway rivers; (b) astronomic tide in Shivering Sands (blue line), with tidal range shown on the second axis (red line).

Since the duration of the simulated period can strongly affect the final results because of the influence of the initial conditions, different types of simulations were run to represent the behaviour during one single month. For this purpose, three single-month simulations were run starting from a regime condition, i.e. a simulation with constant tide and riverine discharge where two consecutive tidal cycles were repeated until they give the same periodic result in terms of salinity distribution. Then, the selected month was simulated twice: the first time as a

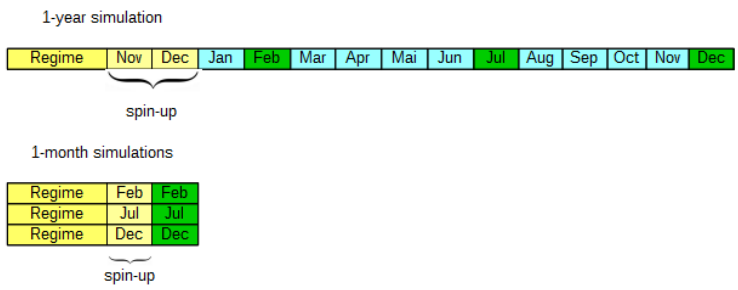


**Fig. 5** Scheme of the simulations that were run for the 1-year and the 1-month approach. Spin-up time was two months.

spin-up period, and the second time to obtain the results to be analysed. The scheme of the simulations is represented in Figure 5.

## 2 Sediment and metal model

Sediments are modelled in Delft3d-WAQ as suspended solids of the type 'inorganic matter' (IM), with particle size defined indirectly through the sedimentation velocity. The particles are eroded or settle depending on the local shear stress $\tau$. The resuspension flux (g m$^{-2}$d$^{-1}$)

$$F_{res} = Z_{res} \max\left\{0, \frac{\tau}{\tau_{c,res}} - 1\right\} \tag{1}$$

occurs only when $\tau$ is larger than the critical value $\tau_{c,res}$, with $Z_{res}$ the erosion coefficient (Partheniades, 1962). The sedimentation flux (g m$^{-2}$d$^{-1}$)

$$F_{sed} = w_s C \max\left\{0, 1 - \frac{\tau}{\tau_{c,sed}}\right\} \tag{2}$$

is calculated only for values of $\tau$ smaller than the critical shear stress $\tau_{c,sed}$, with $w_s$ the sedimentation velocity (m d$^{-1}$) and $C$ the sediment concentration (g m$^{-3}$) in the lower computational cell (Krone, 1962).

Metals are modelled accounting for partitioning, i.e. the distinction of total concentrations into dissolved and adsorbed fractions. The two fractions behave differently, in particular the adsorbed fraction is subjected to the same processes as suspended solids (resuspension and sedimentation), while the dissolved part is only affected by advection and diffusion processes (e.g., de Souza Machado et al., 2016). The dissolved fraction can be derived from the mass balance:

$$f_{df} = \frac{1}{1 + K_p C_{SS}}\,, \tag{3}$$

where $K_p$ is the partition coefficient (m$^3$g$^{-1}$) and $C$ is the concentration of suspended solids. The particulate fraction is calculated as $f_p = 1 - f_{df}$ (e.g., Barreto et al., 2011).

**Table 1** Main numerical parameters and constants used in the implementation of the model Delft3D-FLOW.

| Description | Value | Unit |
|---|---|---|
| Number of grid points 3D simulation | M=915, N=59, K=15 | - |
| Layer thickness from top to bottom | 6.67 | % |
| Time step | 0.2 | min |
| Thatcher-Harleman return time (surface) | 0 (River Thames) | min |
| | 100 (sea boundary) | min |
| | 0 (River Medway) | min |
| Thatcher-Harleman return time (bottom) | 0 (River Thames) | min |
| | 100 (sea boundary) | min |
| | 0 (River Medway) | min |
| Gravitational acceleration | 9.81 | $m/s^2$ |
| Density of water at background temperature and salinity | 1000 | $kg/m^3$ |
| Background water temperature | 15 | $^oC$ |
| Bottom roughness in u-dir. as Chézy | 75-100 ([a]) | $m^{1/2}/s$ |
| Bottom roughness in v-dir. as Chézy | 75-100 ([a]) | $m^{1/2}/s$ |
| Horizontal eddy viscosity | 5-400 ([b]) | $m^2/s$ |
| Horizontal eddy diffusivity | 5-400 ([b]) | $m^2/s$ |

[a] 75 in the first reach from Teddington to London Bridge, then it increases linearly up to 100 in Woolwich and remains constant and equal to this value for the rest of the estuary.
[b] variable from 5 to 400 depending on the grid cell area.

## 3 Implementation of the model

### 3.1 Model parameters

The main numerical parameters and constants used in the implementation of the Delft3D-FLOW module are reported in Table 1. Roughness, expressed through the Chézy coefficient, was assumed 75 $m^{1/2}/s$ in the first reach from Teddington to Tower (coarser sediments), then increasing linearly up to 100 $m^{1/2}/s$ at Woolwich, and remaining constant and equal to this value for the muddy and sandy part of the estuary. These values were determined considering the sediment distribution (Baugh et al., 2013; Prentice, 1972; Mitchell et al., 2012; Lavery and Donovan, 2005) and evaluating the response of the model to changes in these parameters.

It is worth mentioning that for calculating the vertical turbulent eddy viscosity and the vertical turbulent eddy diffusivity the second-order turbulence closure model $k$-$\epsilon$ was chosen. The effect of the horizontal eddy coefficients is discussed in the following section.

The main parameters used for the implementation of Delft3D-WAQ are reported in Tables 2 and 3. Here we note that the sediment availability in the sedimentation layer S1 was observed to influence the concentration of TSS in the water column. To avoid limitation due to the fast emptying of the model's S1 layer, a surface density of inorganic matter ($IM_{S1}$) of $10^3$ $kg/m^2$ was initially imposed, leading to a layer thickness $z = IM_{S1}/\rho_s \sim 0.38$ m, given a solid particle density $\rho_s \simeq 2.6{\cdot}10^3$ $kg/m^3$. Analogously, the initial mass of metals in the sediment layer was estimated by assuming that the ratio $metal_{S1}/IM_{S1}$ is the same as the ratio between metal particulate and IM in the water column, computed with concentrations measured during the year 2006. The calculated values are 20 $g/m^2$ for copper and 100 $g/m^2$ for zinc. The partitioning coefficient $K_p$ was derived from the dataset of 2006. For the cases in which dissolved concentration was greater

**Table 2** Initial conditions used in the implementation of the model Delft3D-WAQ.

| Initial conditions | | |
|---|---|---|
| Description | Value | Unit |
| Inorganic matter in the water column | from restart file | $g/m^3$ |
| Copper in the water column | from restart file | $g/m^3$ |
| Zinc in the water column | from restart file | $g/m^3$ |
| Inorganic matter in S1 layer | $10^6$ | $g/m^2$ |
| Inorganic matter in S2 layer | 0 | $g/m^2$ |
| Copper in S1 layer | 20 | $g/m^2$ |
| Copper in S2 layer | 0 | $g/m^2$ |
| Zinc in S1 layer | 100 | $g/m^2$ |
| Zinc in S2 layer | 0 | $g/m^2$ |

**Table 3** Process parameters and constants used in the implementation of the model Delft3D-WAQ.

| Process parameters | | |
|---|---|---|
| Description | Value | Unit |
| Critical shear stress for sedimentation | 0.2 | $N/m^2$ |
| Sedimentation velocity | 400 | m/day |
| Critical shear stress for resuspension | 0.2 | $N/m^2$ |
| Zero order resuspension flux | 500-5000 ([a]) | $g/(m^2 day)$ |
| Minimum depth for sedimentation | 0.1 | m |
| Partition coefficient Cu in the water column | 7 | $m^2/kg$ |
| Partition coefficient Cu in layer S1 | 7 | $m^2/kg$ |
| Partition coefficient Zn in the water column | 7 | $m^2/kg$ |
| Partition coefficient Zn in layer S1 | 7 | $m^2/kg$ |

[a] Variable along the estuary depending on sediment distribution: from Teddington to London Bridge 500, then a transitional area with linear increase, 5000 from Woolwich to Mucking, transitional area with smooth decrease, and again 500 from Chapman Buoy to the sea boundary.

than total, dissolved concentration was assumed equal to the total within analytic capabilities. The calculated value of $K_p$ is 7 $m^3/kg$ for both metals and was not very sensitive to salinity.

Other water quality parameters were calibrated especially considering the results obtained for the higher temporal resolution dataset in February and August 2011: sedimentation velocity $w_s = 400$ m/day; critical shear stress for sedimentation and resuspension $\tau_{c,sed} = \tau_{c,res} = 0.2$ $N/m^2$. The erosion coefficient $Z_{res}$ was assumed as variable along the estuary depending on sediment distribution: $Z_{res} = 500$ $g/(m^2 day)$ from Teddington to London Bridge, $Z_{res} = 5000$ $g/(m^2 day)$ from Woolwich to Mucking, $Z_{res} = 500$ $g/(m^2 day)$ from Chapman Buoy to the sea boundary; transitional areas with linear variation of $Z_{res}$ assumed among the three previous reaches.

### 3.2 The effect of variable horizontal diffusivity

Horizontal diffusivity and viscosity are assumed identical, with a value variable from 5 to 400 $m^2/s$ depending on the grid cell area $A_g$ ($m^2$) as follows:

$$D_H = \nu_H = \alpha\sqrt{A_g} \tag{4}$$

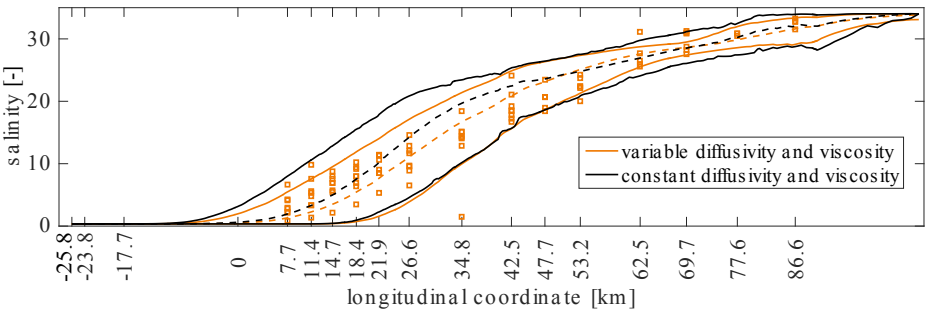


**Fig. 6** Salinity envelopes in February 2006 using variable diffusivity and viscosity and constant values along the estuary. Continuous lines represent minimum and maximum values, dashed lines represent mean values. Measurements are reported as coloured squares.

with $\alpha = 0.1$ m/s. In fact, the amount of mixing that has to be included in the model depends on the grid size because it is correlated with eddy size, which affects the diffusion coefficient (Okubo, 1971), possibly influencing hydrodynamics and transport processes (Toffolon and Rizzi, 2009; Toffolon, 2013). The assumption of variable values throughout the estuary is necessary to obtain realistic longitudinal profiles of salinity.

Here we report a comparison between two identical simulations run in February 2006 with different values of diffusivity and viscosity (Figure 6). In the first case, the variable values as in the current study are used, while in the second example the default constant values suggested by the Delft3D model are kept, e.g. a horizontal diffusivity of 10 $m^2$/s and a horizontal viscosity of 1 $m^2$/s.

It is interesting to notice that the simulation with variable coefficients leads to a more regular shape of the envelope, consistent with available measurements. Conversely, constant values of diffusivity and viscosity lead to an envelope with an unrealistic change of slope in the middle of the estuary.

## 4 Evaluation of model performances

Table 4 reports the values of the correlation coefficient and the Root Mean Square Error (RMSE) for modelled and measured water level, salinity, TSS and metals concentrations. The table refers to Figure 5 in the main text.

As shown in Figure 4a in the main text, modelled and observed water level present a very good agreement except for few limited points. These outliers are clearly due to erroneous acquisition by the tidal gauge system, in fact they show a constant value for the observed water level. Since the data did not have any quality flag, we did not exclude these potentially wrong acquisitions, which however do not affect the overall good agreement as they are few acquisitions compared to the long time-series we used. Two examples for Silvertown and Tower are shown in Figure 7 and 8, respectively.

**Table 4** Correlation coefficient and RMSE for modelled and measured water level, salinity, TSS and metal concentrations.

| | Corr. coeff. | RMSE |
|---|---|---|
| WL Richmond | 0.904 | 0.620 m |
| WL Tower | 0.962 | 0.535 m |
| WL Silvertown | 0.970 | 0.499 m |
| WL Tilbury | 0.977 | 0.404 m |
| WL Denton | 0.965 | 0.511 m |
| WL Coryton | 0.981 | 0.356 m |
| WL Southend | 0.982 | 0.325 m |
| WL Sheerness | 0.982 | 0.311 m |
| Salinity | 0.982 | 2.52 |
| TSS | 0.513 | 65.4 mg/L |
| Copper | 0.812 | 1.86 $\mu$g/L |
| Zinc | 0.825 | 7.34 $\mu$g/L |

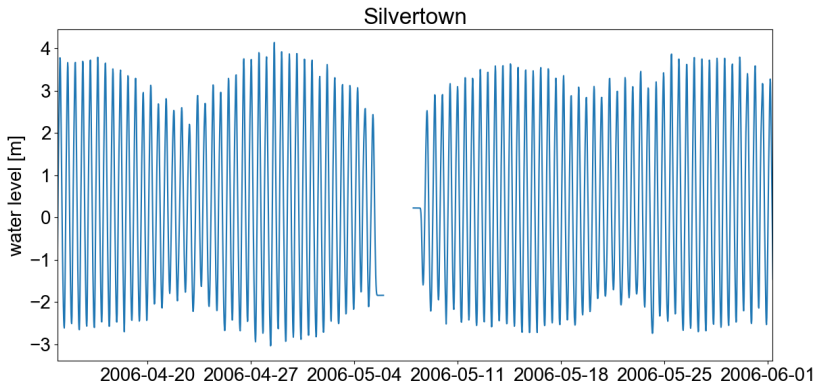


**Fig. 7** Details of some acquisition problems for the tidal gauge in Silvertown.

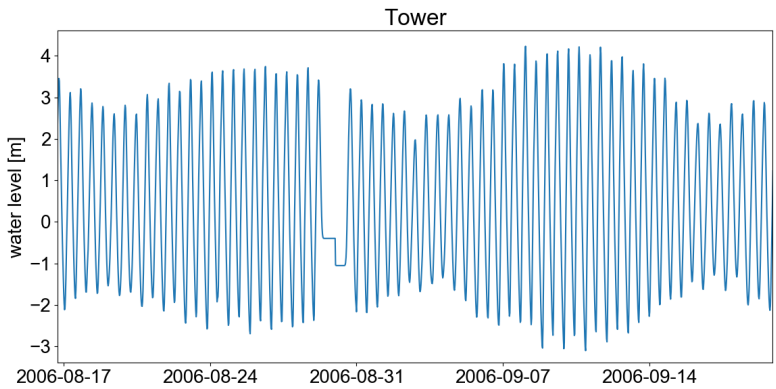


**Fig. 8** Details of some acquisition problems for the tidal gauge in Tower.

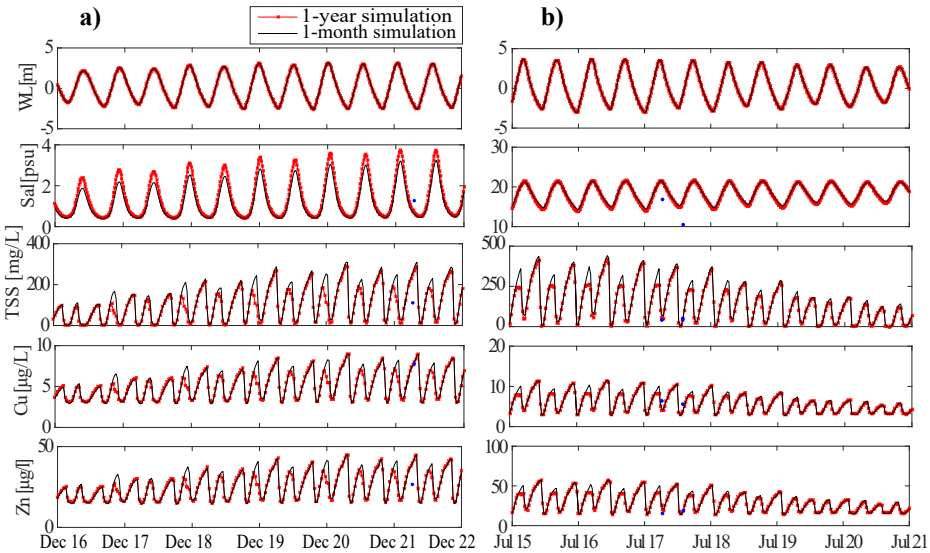


**Fig. 9** Comparison between one-year (dotted line) and single-month (continuous line) simulations in Erith for: (a) December 2006 and (b) July 2006. Blue dots represent measurements.

## 5 Duration of the simulation

To show how important the duration of the simulated period can be, a comparison was made between the one-year simulation and three single-month cases (February, July and December, characterized by mid, low and high river discharge, respectively). Differences can be seen especially in the salinity and water quality results. As an example, we analysed the behaviour in July and December 2006, when the freshwater discharge was different, in the central location of Erith (Figure 9). In December, the salinity significantly differs between the two simulations, and the single-month simulation underestimates the salinity (i.e., predicts a shorter salt intrusion in the estuary), which in turn also modifies the TSS and metal concentrations (Figure 9a). Conversely, for the dry month (July) the differences are irrelevant, with only small discrepancies reported for TSS and metals (Figure 9b).

## References

Barreto SRG, Barreto WJ, Deduch EM (2011) Determination of partition coefficients of metals in natural tropical water. CLEAN–Soil, Air, Water 39(4):362–367

Baugh J, Feates N, Littlewood M, Spearman J (2013) The fine sediment regime of the Thames Estuary–A clearer understanding. Ocean & coastal management 79:10–19

Krone RB (1962) Flume studies of the transport of sediment in estuarial shoaling processes

Lavery S, Donovan B (2005) Flood risk management in the Thames Estuary looking ahead 100 years. Philosophical Transactions of the Royal Society of London A: Mathematical, Physical and Engineering Sciences 363(1831):1455–1474

Mitchell S, Akesson L, Uncles R (2012) Observations of turbidity in the Thames estuary, United Kingdom. Water and Environment Journal 26(4):511–520

Okubo A (1971) Oceanic diffusion diagrams. In: Deep sea research and oceanographic abstracts, Elsevier, vol 18, pp 789–802

Partheniades E (1962) A study of erosion and deposition of cohesive soils in salt water. University of California, Berkeley

Prentice JE (1972) Sedimentation in the inner estuary of the Thames, and its relation to the regional subsidence. Philosophical Transactions of the Royal Society of London Series A, Mathematical and Physical Sciences 272(1221):115–119

de Souza Machado AA, Spencer K, Kloas W, Toffolon M, Zarfl C (2016) Metal fate and effects in estuaries: A review and conceptual model for better understanding of toxicity. Science of The Total Environment 541:268–281

Toffolon M (2013) Ekman circulation and downwelling in narrow lakes. Adv Water Resour 53:76–86

Toffolon M, Rizzi G (2009) Effects of spatial wind inhomogeneity and turbulence anisotropy on circulation in an elongated basin: a simplified analytical solution. Adv Water Resour 32:1554–1566